Mechanism Reduction and Generation Using Analysis of Major Fuel Consumption Pathways for *n*-Heptane in Premixed and Diffusion Flames

Hongzhi R. Zhang,* Eric G. Eddings, and Adel F. Sarofim

Department of Chemical Engineering, University of Utah, Salt Lake City, Utah 84112

Charles K. Westbrook

Chemical and Nuclear Science Division, Lawrence Livermore National Laboratory, Livermore, California 94551

Received February 28, 2006. Revised Manuscript Received April 17, 2007

Reaction pathway analyses were conducted for three mechanisms (designated as the Pitsch, Utah, and Lawrence Livermore National Lab) for a normal heptane premixed flame ($\Phi = 1.9$) and a normal heptane opposed diffusion flame, in order to identify the relative importance of the major fuel consumption pathways in the two flame classes. In premixed flames, hydrogen abstraction is found to be the major fuel consumption route although it is surpassed by thermal decomposition when the flame temperature exceeds 1400−1500 K. At the higher temperatures, however, little fuel remains in a premixed flame so that thermal decomposition provides a minor pathway for overall fuel decomposition. The principal abstractor is the hydrogen radical in all three mechanisms with the hydroxyl radical having a secondary role. In opposed diffusion flames, thermal decomposition competes with hydrogen abstraction in providing the major pathway for fuel consumption. Thermal decomposition becomes important when a large fraction of the fuel reaches the high-temperature zone in a flame. By understanding the relative importance of competing fuel consumption pathways, mechanisms can be tailored to each specific application by eliminating or lumping insignificant reactions. The results obtained in this study for *n*-heptane may be used to guide the reduction of existing mechanisms for a particular application or the generation of mechanisms for the combustion of larger paraffins that are major components of liquid aviation and transportation fuels.

Introduction

Heptane combustion chemistry provides the foundation for mechanisms of higher hydrocarbon species such as decane, dodecane, and cetane found in commercial fuels. Detailed mechanisms of large paraffins are of formidable sizes that are difficult to apply in modeling efforts of practical flames. In order to guide the simplification of an existing reaction mechanism or the generation of a new mechanism for a higher hydrocarbon, it is useful to identify the reaction classes of greatest importance, and their dependence on combustion environments. As the best studied large paraffin, *n*-heptane is selected for reaction pathway analysis to discover the most important reaction routes for fuel decomposition, formation, and consumption of olefins, evolution of intermediates, and formation of major products.

Heptane is a primary reference fuel for spark ignition engines and has been studied exhaustively. Some recent experimental[1−12] and modeling[13−21] results on *n*-heptane combustion are summarized in Tables 1 and 2. The combustion of *n*-heptane and other large *n*-paraffins includes a low-temperature region, in which alkylperoxy radical chemistry dominates, and a high-temperature region controlled by fuel and large radical pyrolysis and oxidation that generate intermediates that react rapidly to produce C_2-C_4 species. Dagaut et al.[2] identified 750 K as the temperature separating the low- and high-temperature regimes

* Corresponding author. E-mail: westshanghai@yahoo.com.

(1) Burcat, A.; Farmer, R. C.; Matula, R. A. *Proc. 13th Int. Symp. Shock Tubes Shock Waves* **1981**, *13*, 826.

(2) Dagaut, P.; Reuillon, M.; Cathonnet, M. Experimental study of the oxidation of *n*-heptane in a jet stirred reactor from low to high temperature and pressures up to 40 atm. *Combust. Flame* **1995**, *101*, 132.

(3) Simon, Y.; Scacchi, G.; Baronnet, F. Studies on the oxidation reactions of *n*-heptane and isooctane. *Can. J. Chem.* **1996**, *74*, 1391.

(4) Minetti, R.; Carlier, M.; Ribaucour, M.; Therssen, E.; Sochet, L. R. Comparison of oxidation and autoignition of the two primary reference fuels by rapid compression. *Proc. Combust. Inst.* **1996**, *26*, 747.

(5) Doute, C.; Delfau, J. L.; Akrich, R.; Vovelle, C. Experimental study of the chemical structure of low-pressure premixed *n*-heptane−O2−Ar and isooctane−O2−Ar flames. *Combust. Sci. Technol.* **1997**, *124*, 249.

(6) Seiser, R.; Truett, L.; Trees, D.; Seshadri, K. Structure and extinction of non-premixed *n*-heptane flames. *Proc. Combust. Inst.* **1998**, *27*, 649.

(7) El Bakali, A.; Delfau, J. L.; Vovelle, C. Experimental study of 1 atmosphere, rich, premixed *n*-heptane and iso-octane flames. *Combust. Sci. Technol.* **1998**, *140*, 69.

(8) El Bakali, A.; Delfau, J. L.; Vovelle, C. Kinetic modeling of a rich, atmospheric pressure, premixed *n*-heptane/O2/N2 flame. *Combust. Flame* **1999**, *118*, 381.

(9) Ingemarsson, A. T.; Pedersen, J. R.; Olsson, J. O. Oxidation of *n*-heptane in a premixed laminar flame. *J. Phys. Chem. A* **1999**, *103* (41), 8222.

(10) Colket, M. B., III; Spadaccini, L. J. Scramjet fuels autoignition study. *J. Prop. Power* **2001**, *17*, 315.

(11) Vovelle, C. Personal communication, 2001.

(12) McEnally, C. S.; Ciuparu, D. M.; Pfefferle, L. D. Experimental study of fuel decomposition and hydrocarbon growth processes for practical fuel components: heptanes. *Combust. Flame* **2003**, *134* (4), 339−353.

(13) Lindstedt, R. P.; Maurice, L. Q. Detailed kinetic modeling of *n*-heptane combustion. *Combust. Sci. Technol.* **1995**, *107* (4−6), 317−353.

(14) Bollig, M.; Pitsch, H.; Hewson, J. C.; Seshadri, K. Reduced *n*-heptane mechanism for non-premixed combustion with emphasis on pollutant-relevant intermediate species. *Proc. Combust. Inst.* **1996**, *26*, 729.

10.1021/ef060092z CCC: $37.00
Published on Web 06/01/2007

Table 1. Experimental Results on *n*-Heptane Oxidation

investigators	apparatus	exp conditions	measurement
Burcat et al.[1]	shock tube	$\Phi = 1$	ignition delay
Dagaut et al.[2]	well stirred reactor	high pressure, $T = 550-1150$ K, $\Phi = 1$, $\tau = 0.1-2$ s	50 species
Simon et al.[3]	well stirred reactor	subatmospheric, $T = 923$ K, $\tau = 0.1-0.9$ s	16 species
Minetti et al.[4]	rapid compression machine	$T = 645-890$ K	concentration of intermediates and ignition delay
Doute et al.[5]	premixed flame	$P = 6$ kPa, $\Phi = 0.7-2.0$	species profiles
Seiser et al.[6]	counter-flow diffusion	non-premixed	extinction and a dozen species
El Bakali et al.[7]	premixed flame	760 Torr, $\Phi = 1.9$	two dozen species
El Bakali et al.[8]	premixed flame	760 Torr, $\Phi = 1.9$	two dozen species, including isomers
Ingemarsson et al.[9]	premixed flame	760 Torr, $\Phi = 1$	18 species
Colket and Spadaccini[10]	shock tube	$T = 1100-1500$ K, $P = 3-8$ atm, $\Phi = 0.5-1.5$	ignition delay
Vovelle et al.[11]	premixed flame	760 Torr, $\Phi = 1.0, 1.5$	two dozen species
McEnally et al.[12]	coflowing flame	non-premixed methane flames doped with heptanes	soot volume fraction, species concentrations

Table 2. Models for *n*-Heptane Oxidation

investigators	rxns	species	systems modeled	classes of compounds	comment
Lindstedt and Maurice[13]	659	109	counter-flow diffusion flame, stirred reactor, and premixed flame	olefin, alkane, benzene	well predicted species concentrations and flame temperatures; abstraction and thermal decomposition are major fuel consumption pathways in diffusion flames
Pitsch et al.[14]	77	38	counter-flow diffusion flame	olefin, alkane	determined that thermal decomposition can account for 30% of *n*-heptane consumption
Held et al.[15]	266	39	flow reactor, stirred reactor, shock tube, premixed flame speed	olefin, alkane, propyne, benzene	found to provide best fit of laminar flame speed by Davis and Law;[16] found to provide the best agreement with Davidson et al.[17] ignition delay measurement at reflected shock waves
Ranzi et al.[18]	7000	260	premixed flames	olefin, alkane, alkyne, diene, aromatics, PAH, carbonyl compound	lumped reactions used; each reaction can have multiple reactants and products; verified for *n*-heptane, iso-octane,[18] and kerosene[19] flames
Curran et al.[20]	2500	561	rapid compression machine, shock tubes, well stirred reactor, high-pressure flow reactor	olefin, alkane, alkyne, diene, carbonyl compound	detailed low-temperature chemistry, and extensively tested in low-temperature applications
Doute et al.[21]	550	65	four 6 kPa and one atmospheric premixed flame	olefin, alkane, alkyne, diene, benzene	most stable species were well predicted; the model was also able to predict the concentrations of active radicals for rich flames

based on their high-pressure, jet stirred reactor experiments of *n*-heptane oxidation, and most experimental and kinetic modeling studies, such as that of Ciezki and Adomeit,[22] observe a transition between the high- and low-temperature regimes between about 700 and 850 K. While the low-temperature oxidation regime has a considerable impact on fuel autoignition[23] and phenomena including engine knock, low-temperature oxidation reaction paths are usually considered to have little influence on premixed or non-premixed flame properties. One goal of this paper is to compare flame models with and without these low-temperature reaction pathways, in order to assess their role and importance and the impacts of ignoring them in reduced kinetic models for flame propagation.

In this paper, the combustion of normal heptane will be investigated in both premixed and diffusion flames. Because of the chemical similarity between species in a homologous series such as *n*-alkanes, understanding the major reaction classes of heptane and the major reaction product distributions should suggest a universal pattern of combustion chemistry for longer *n*-paraffins. Use of the information obtained from reaction pathway analysis in *n*-heptane for mechanism reduction in any large *n*-alkane will also be discussed.

In order to evaluate the importance of reaction pathways, three different *n*-heptane mechanisms were selected for study. While all three mechanisms were produced by selectively reducing a large, extremely detailed kinetic mechanism, their reductions were chosen to accomplish different objectives, and all three have been reduced by different amounts. Comparisons are made between all three mechanisms with selected experimental premixed and opposed flow diffusion flame data in the literature to provide a benchmarking of the models. The major intent of the study is not to select the "best" model but to use the different

(15) Held, T. J.; Marchese, A. J.; Dryer, F. L. A semi-empirical reaction mechanism for *n*-heptane oxidation and pyrolysis. *Combust. Sci. Technol.* **1997**, *123*, 107.

(16) Davis, S. G.; Law, C. K. Laminar flame speeds and oxidation kinetics of iso-octane−air and *n*-heptane−air flames. *Proc. Combust. Inst.* **1998**, *27*, 521.

(17) Davidson, D. F.; Horning, D. C.; Hanson, R. K.; Hitch, B. Shock tube ignition time measurements for n-heptane/O2/Ar with and without additives. Presented at the 22nd International Symposium on Shock Waves, London, July 18−23, 1999; paper 360.

(18) Ranzi, E.; Faravelli, T.; Gaffuri, P.; Sogaro, A.; Danna, A.; Ciajolo, A. A wide-range modeling study of iso-octane oxidation. *Combust. Flame* **1997**, *108*, 24.

(19) Violi, A.; Yan, S.; Eddings, E. G.; Sarofim, A. F.; Granata, S.; Faravelli, T.; Ranzi, E. Experimental formulation and kinetic model for JP-8 surrogate mixtures. *Combust. Sci. Technol.* **2002**, *174*, 399.

(20) Curran, H. J.; Gaffuri, P.; Pitz, W. J.; Westbrook, C. K. A comprehensive modeling study of *n*-heptane oxidation. *Combust. Flame* **1998**, *114*, 149.

(21) Doute, C.; Delfau, J. L.; Vovelle, C. Detailed reaction mechanisms for low pressure premixed *n*-heptane flames. *Combust. Sci. Technol.* **1999**, *147*, 61.

(22) Ciezki, H. K.; Adomeit, G. Shock-Tube Investigation of Self-Ignition of *n*-Heptane−Air Mixtures under Engine Relevant Conditions. *Combust. Flame* **1993**, *93*, 421−433.

(23) Westbrook, C. K. Chemical Kinetics of Hydrocarbon Ignition in Practical Systems. *Proc. Combust. Inst.* **2000**, *28*, 1563−1577.

models to obtain insights on the dominant reaction pathways predicted by each model to assist in mechanism reduction.

Experimental Data and Numerical Models

The three mechanisms chosen for the pathway analyses are the following:

- *LLNL mechanism.* A detailed heptane mechanism[24] reduced from a complete set proposed by Curran et al.[20] at Lawrence Livermore National Laboratory (LLNL) that includes approximately 160 species and 1500 reactions for both low- and high-temperature chemistry.
- *Pitsch mechanism.* A smaller Pitsch[25] *n*-heptane model extended from an earlier publication[14] with both high-temperature oxidation and low-temperature peroxy radical reactions. This remarkably efficient mechanism with only 112 reactions and 44 species requires much less resources to run than its larger LLNL counterpart.
- *Utah mechanism.* A relatively small mechanism compiled at the University of Utah with 187 species and 932 reactions based on submodules of hydrogen,[26] acetylene,[27−29] acetylene set with vinyl and aromatic radicals,[30] ethylene,[31] propane,[32] propylene,[33] *n*-butane,[34] benzene formation,[35] toluene and benzene oxidation,[36] *n*-heptane,[21] and isooctane.[37] The compilation is named the Utah heptane mechanism; it is the core mechanism that has been extended to build up a JP8 mechanism in our recent publication.[38]

All three reduced mechanisms were tested using experimental data of two very different types of flames, in order to evaluate the effects of flame type on the important kinetic reaction pathways. The experiments included a laminar, atmospheric-pressure, premixed *n*-heptane flame with an equivalence ratio of 1.9,[8] and a non-premixed, atmospheric-pressure, *n*-heptane, opposed-flow diffusion flame[6] with a strain rate of 150 1/s (fuel side 15% *n*-heptane and 85% N_2 at 338 K, 34.2 cm/s; air side at 298 K, 37.5 cm/s). All three of the mechanisms above were used to simulate the premixed flame, and the opposed-flow diffusion flame was modeled using the Pitsch mechanism. The Pitsch mechanism was selected because of its ability to fit the major features of product formation and fuel consumption with a relatively small set of reactions.

The numerical model used for this study was CHEMKIN III,[39] and the thermodynamic data were obtained from the CHEMKIN thermodynamic database[40] or estimated by THERGAS[41] employing Benson's group additivity theory.[42] The transport properties of species were obtained from the CHEMKIN transport database[43] or estimated from the transport properties of similar species.

Comparative Mechanism Reaction Pathway Analysis

The computed predictions of fuel and oxygen consumption rates were compared with the experimental values and used in this study to adjust temperature profiles, using techniques that were discussed in an earlier publication.[44] The resulting predicted concentration profiles of the fuel, oxidant, and major gaseous products in the premixed *n*-heptane/O_2/N_2 flame (Φ = 1.9) of El Bakali et al.[8] are shown in Figure 1. Additional comparisons of concentrations of selected olefins with measured experimental profiles of the same *n*-heptane flame were presented in an earlier study.[45] All three mechanisms are able to reproduce the measured concentration profiles of most major gaseous products. The predicted concentration profiles of selected major species in the opposed diffusion flame[6] using the Pitsch mechanism are illustrated in Figure 2. The model gives good agreement with the measured rates of fuel consumption and major product formation.

Two major reaction classes are responsible for the consumption of *n*-heptane in these flames: one reaction class is thermal decomposition of the *n*-alkane fuel molecule, which forms two alkyl radicals after the rupture of a C−C σ bond; the other is hydrogen abstraction from the *n*-alkane fuel by a radical species, which breaks a C−H σ bond to form a conjugate alkyl radical. The alkyl radicals produced via both reaction classes then decompose via β scission to form a smaller alkyl radical plus an olefin species. In the low-temperature oxidation regime, alkyl radicals can react via addition of molecular oxygen to produce alkylperoxy radicals which lead to so-called "cool flames", but these processes do not contribute to the flame structure of any of the flames examined in this study, although they do have some impact on predicted OH radical levels, as discussed below.

In the following sections, the reaction pathways for hydrogen abstraction and thermal decomposition are compared for the three different mechanisms. The resulting information will identify the dominant pathways for fuel consumption and will

(24) Seiser, R.; Pitsch, H.; Seshadri, K.; Pitz, W. J.; Curran, H. J. Extinction and autoignition of *n*-heptane in counterflow configuration. *Proc. Combust. Inst*. **2000**, *28*, 2029.
(25) Liu, S.; Hewson, J. C.; Chen, J. H.; Pitsch, H. Effects of strain rate on high-pressure nonpremixed *n*-heptane autoignition in counterflow. *Combust. Flame* **2004**, *137* (3), 320−339.
(26) Marinov, N. M.; Westbrook, C. K.; Pitz, W. J. Detailed and global kinetics model for hydrogen. In *Transport Phenomena in Combustion*; Chan, S. H., Ed.; Taylor & Francis: Washington, DC, 1996; Vol. 1, pp 118−129.
(27) Hwang, S. M.; Gardiner, W. C., Jr.; Frenklach, M.; Hidaka, Y. Introduction zone exothermicity of acetylene ignition. *Combust. Flame* **1986**, *67*, 65.
(28) Miller, J. A.; Mitchell, R. E.; Smooke, M. D.; Kee, R. J. Toward a comprehensive chemical kinetic mechanism for the oxidation of acetylenes comparison of model predictions with results from flame and shock tube experiments. *Proc. Combust. Inst.* **1982**, *19*, 181.
(29) Westbrook, C. K. Chemical kinetics of hydrocarbon oxidation in gaseous detonations. *Combust. Flame* **1982**, *46*, 191.
(30) Wang, H.; Frenklach, M. Calculations of rate coefficients for the chemically activated reactions of acetylene with vinylic and aromatic radicals. *J. Phys. Chem.* **1994**, *2*, 11465.
(31) Marinov, N. M.; Malte, P. C. Ethylene oxidation in a well-stirred reactor. *Int. J. Chem. Kinet.* **1995**, *27*, 957.
(32) Tsang, W. Chemical kinetics data base for combustion chemistry. Part 2. Propane. *J. Phys. Chem. Ref. Data* **1988**, *17*, 887.
(33) Tsang, W. Chemical kinetics data base for combustion chemistry. Part 5. Propene. *J. Phys. Chem. Ref. Data* **1991**, *20*, 221.
(34) Pitz, W. J.; Westbrook, C. K.; Leppard, W. K. *Autoignition chemistry of C_4 olefins under motored engine conditions: a comparison of experimental and modeling results*; SAE paper no. 912315, Society of Automotive Engineers, Warrendale, Pa, 1991.
(35) Miller, J. A.; Melius, C. F. Kinetic and thermodynamic issues in the formation of aromatic compounds in flames of aliphatic fuels. *Combust. Flame* **1992**, *91*, 21.
(36) Emdee, J.; Brezinsky, K.; Glassman, I. A Kinetic model for the oxidation of toluene near 1200 K. *J. Phys. Chem.* **1992**, *96*, 2151.
(37) Pitsch, H.; Peters, N.; Seshadri, K. Numerical and asymptotic studies of the structure of premixed isooctane flames. *Proc. Combust. Inst.* **1996**, *26*, 763.
(38) Zhang, H. R.; Eddings, E. G.; Sarofim, A. F. Criteria for Selection of Components for Surrogate of Natural Gas and Transportation Fuels. *Proc. Combust. Inst.* **2007**, *31*, 401−409.
(39) Kee, R. J.; Rupley, F. M.; Miller, J. A.; Coltrin, M. E.; Grcar, J. F.; Meeks, E.; Moffat, H. K.; Lutz, A. E.; Dixon-Lewis, G.; Smooke, M. D.; Warnatz, J.; Evans, G. H.; Larson, R. S.; Mitchell, R. E.; Petzold, L. R.; Reynolds, W. C.; Caracotsios, M.; Stewart, W. E.; Glarborg, P.; Wang, C.; Adigun, O.; Houf, W. G.; Chou, C. P.; Miller, S. F. *Chemkin collection*, release 3.7.1; Reaction Design, Inc: San Diego, CA, 2003.
(40) Kee, R. J.; Rupley, F. M.; Miller, J. A. *The Chemkin thermodynamic database*; Sandia Report #SAND 87-8215B, 1993.
(41) Muller, C.; Michel, V.; Scacchi, G.; Côme, G. M. THERGAS: a computer program for the evaluation of thermochemical data of molecules and free radicals in the gas phase. *J. Chim. Phys.* **1995**, *92*, 1154.
(42) Benson, S. W.; Cruickshank, F. R.; Golden, D. M.; Haugen, G. R.; O'Neal, H. E.; Rodgers, A. S.; Shaw, R.; Walsh, R. *Chem. Rev.* **1969**, *69*, 279.
(43) Kee, R. J.; Dixon-Lewis, G.; Warnatz, J.; Coltrin, M. E.; Miller, J. A. *The Chemkin transport database*; Sandia Report #SAND 86-8246, 1986.
(44) Zhang, H. R.; Eddings, E. G.; Sarofim, A. F. Combustion Reactions of Paraffin Components in Liquid Transportation Fuels Using Generic Rates. *Combust. Sci. Technol.* **2007**, *179* (1−2), 61−89.
(45) Zhang, H. R.; Eddings, E. G.; Sarofim, A. F. Olefin Chemistry in a Premixed Heptane Flame. *Energy Fuels* **2007**, *21* (2), 677−685.

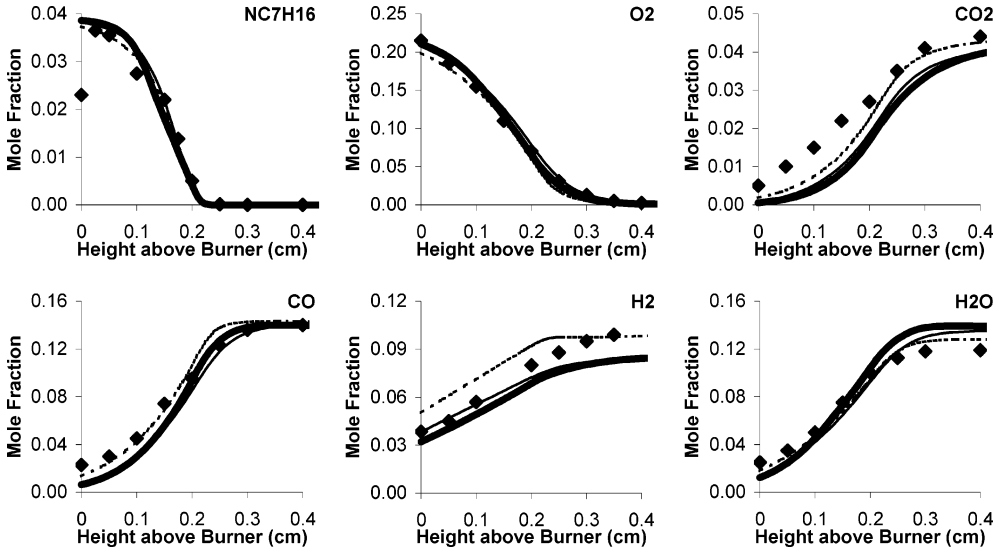

Figure 1. Comparison between numerical results and experimental data for the fuel, oxidant, and major gaseous products of the premixed *n*-heptane flame ($\Phi = 1.9$),[8] using the LLNL reduced mechanism (heavy solid lines), the Utah heptane mechanism (light solid lines), and the Pitsch mechanism (dotted lines).

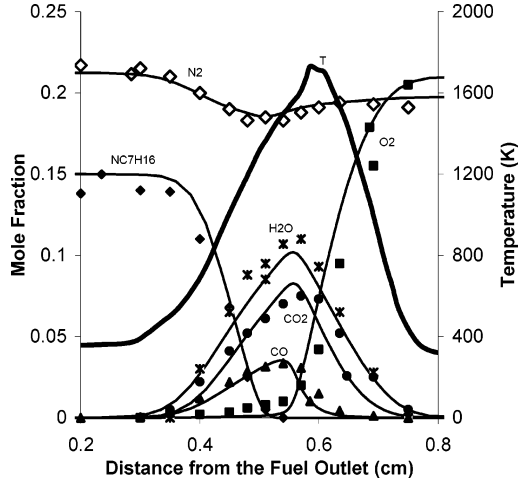

Figure 2. Comparison between experimental data (symbol) and simulation results (line with a corresponding symbol) for selected species of the opposed diffusion flame.[6]

contribute to the product-distribution weighted technique for mechanism reduction.

Fuel Consumption via Hydrogen Abstraction. *Hydrogen Abstraction in Premixed Flames*. The *n*-heptane fuel consists structurally of a long, straight chain of seven C atoms. The two ends of the molecule have methyl (CH_3) radicals, with a series of five CH_2 groups in the center region. The C−H bond strengths are stronger in the CH_3 groups than in the CH_2 groups; the C−H bonds in the methyl radical are called "primary" C−H bonds, and the corresponding bonds in the CH_2 group are called "secondary" C−H bonds.[20] The heptyl radicals that are produced by abstracting an H atom from a primary bond can be called "primary heptyl radicals", and those produced by abstracting an H atom from a secondary bond are collectively called "secondary heptyl radicals". There is only one heptyl radical that can be termed a primary heptyl radical, but there are three structurally distinct secondary heptyl radicals. The magnitudes of the rates of hydrogen abstraction reactions in the premixed flame of Figure 1 are illustrated in Figure 3, as well as the reaction fluxes of carbon atoms through each heptyl radical isomer. The Pitsch mechanism has been simplified by combining all of the secondary heptyl radicals, so it considers only two *n*-heptyl radical isomers, the primary (PXC_7H_{15}) and the secondary (SXC_7H_{15}). The more detailed mechanisms, the LLNL and the Utah mechanisms, distinguish all four possible *n*-heptyl radical isomers denoted by the primary isomer C_7H_{15}-1, and the C_7H_{15}-2, C_7H_{15}-3, and C_7H_{15}-4 secondary isomers. As seen in Figure 3, the formation rate of both C_7H_{15}-2 or C_7H_{15}-3 (for structural reasons, the formation rates of these two isomers are exactly the same) is greater than those of the other two isomers. C_7H_{15}-1 and PXC_7H_{15} are minor products as a result of the stronger primary C−H bonds.

The production rates of the different heptyl radicals are influenced by the temperature and multiplicity of H atoms at each type of site. As the temperature increases, it becomes relatively easier to abstract primary H atoms with their higher bond energies. However, the increasing contribution of the primary radical formation occurs at high enough temperatures that its importance is displaced by the growing rates of thermal decomposition of the parent fuel via breaking C−C bonds, a competing fuel consumption pathway that will be discussed below.

The LLNL mechanism gives unique bimodal rate profiles with one peak at 700 K (minor) and another at 1275 K (major). In contrast to the Utah mechanism, the formation rate of C_7H_{15}-1 is the lowest of those of heptyl radicals for the LLNL mechanism, only surpassing that of C_7H_{15}-4 at 1410 K, and C_7H_{15}-1 formation never dominates at high temperatures. The peak at 700 K is due to the inclusion of low-temperature reaction pathways in the LLNL mechanism.

Hydrogen Abstraction in Opposed Diffusion Flames. In order to study the major fuel consumption pathways for different combustion configurations, the Pitsch mechanism was used to model an *n*-heptane, opposed-flow diffusion flame.[6] As seen in Figure 2, the flame reaches its highest temperatures at 0.58−0.61 cm from the fuel outlet and the most fuel is consumed on the fuel side of the temperature peak. Figure 4 demonstrates striking differences of the major fuel consumption pathways between opposed diffusion and premixed flames (Figure 3) in terms of thermal decomposition (to be discussed later) and primary heptyl radical formation. The primary heptyl radical is formed at a maximum rate of 1.01×10^{-4} mol/(mL s) compared to that of the secondary radical formation of 1.40×10^{-4} mol/(mL s) using the Pitsch mechanism. The net formation rate of

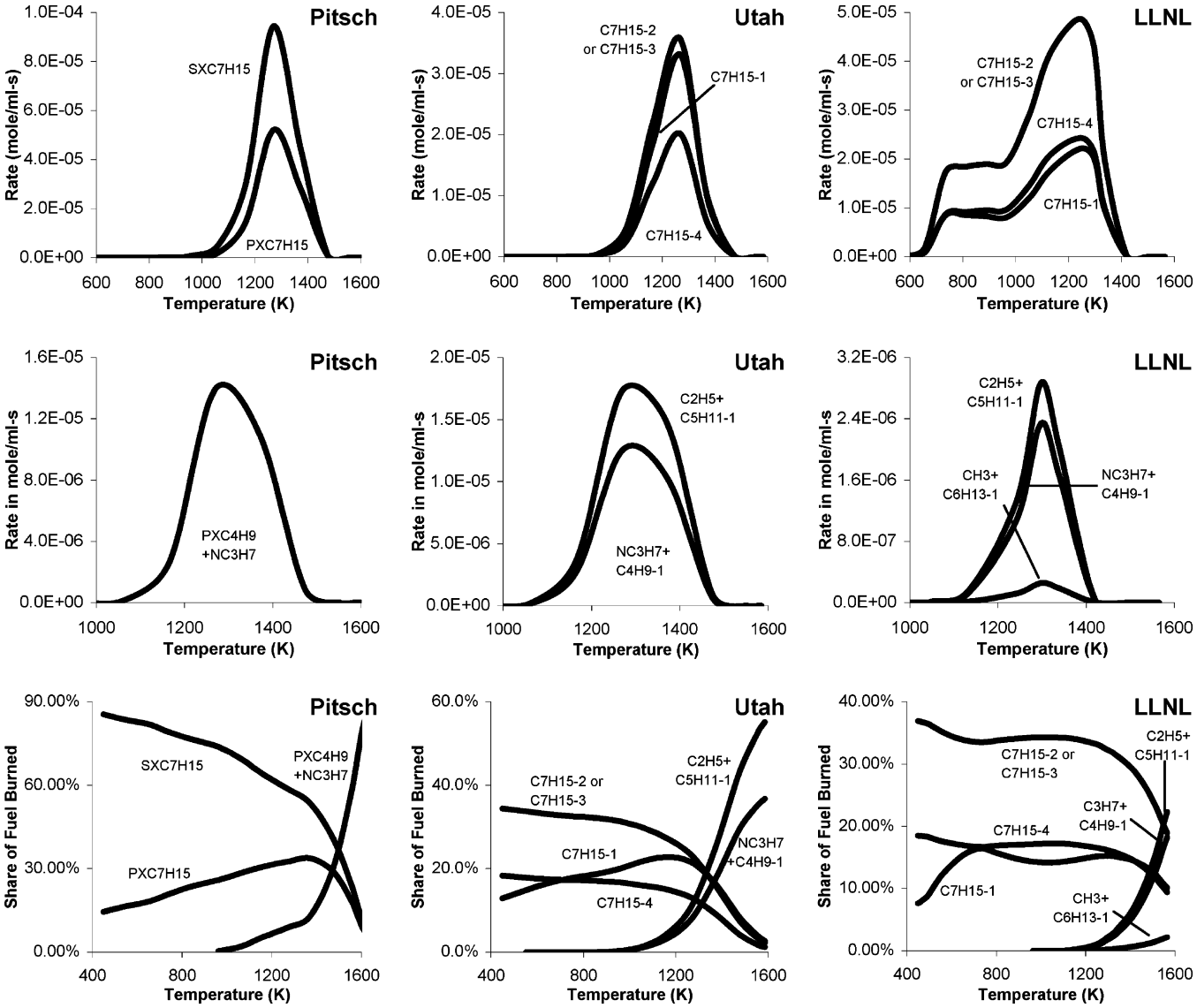

Figure 3. Rates of hydrogen abstraction (first row), thermal decomposition (second row) reactions forming different heptyl radicals in the premixed flame, and their contributions in the fuel consumption process (third row). Share of fuel burned is defined to be the reaction rate of a hydrogen abstraction or a thermal pathway over the total fuel consumption rate that includes both hydrogen abstraction and thermal decomposition.

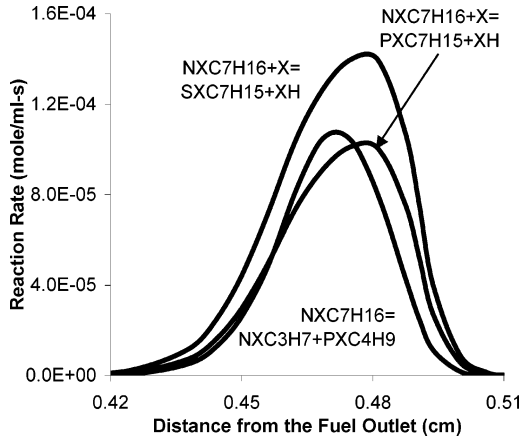

Figure 4. Reaction rates for hydrogen abstraction and thermal decomposition reactions in the opposed diffusion flame.

the secondary radical is only 40% higher than that of the primary radical compared to it being 88% higher in premixed flames using the Pitsch mechanism (Figure 3).

Hydrogen Abstractors. The contributions of H, OH, and other radicals in the fuel consumption process via hydrogen abstraction are important factors in reduction of large mechanisms of paraffinic fuels. For further reduced and beyond skeletal mechanisms, even the contribution of H and OH radicals is critically examined.

Each mechanism employs a different set of hydrogen abstractors. Of the four abstractors used in the Pitsch mechanism, H and OH are most important (Figure 5) reacting at rates 2−4 orders of magnitude faster in both flame configurations than the other two abstractors, HO_2 and O_2, except at temperatures lower than 900 K where hydrogen abstraction reactions by HO_2 radicals are the fastest, because concentrations of HO_2 are greatest at lower temperatures. Hydrogen abstraction reactions by OH radicals are the fastest at low temperatures but are overtaken by reactions by H radicals when the temperature exceeds 1100 K. OH radicals abstract a secondary hydrogen three times faster than a primary one for the Pitsch mechanism. If an H radical is the abstractor, a secondary hydrogen atom is abstracted at a rate 30% faster than a primary one. In contrast to premixed flames, the important contribution of abstraction reactions by OH radicals toward the formation rate of the secondary heptyl radical is not seen in the opposed-flow diffusion flame. Under all conditions examined, hydrogen

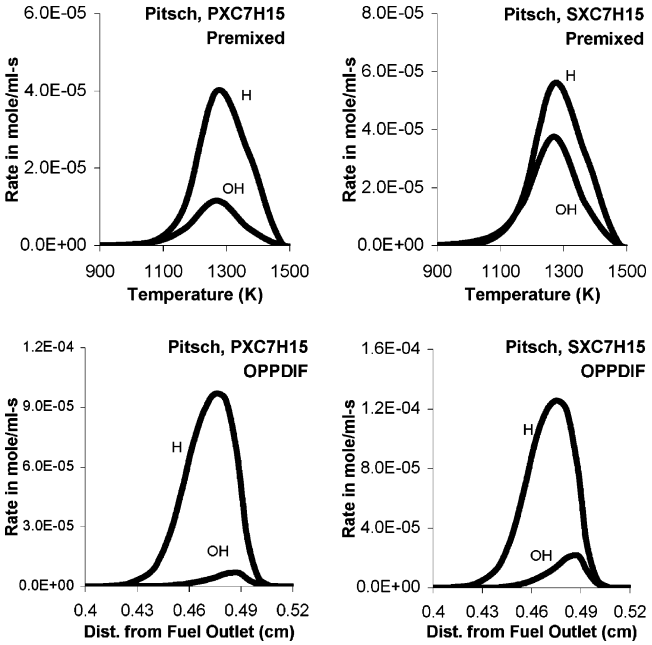

Figure 5. Hydrogen abstraction reaction rates in the premixed flame (first row) and the opposed diffusion flame (second row) using the Pitsch mechanism. H and OH radicals are the major hydrogen abstractors.

abstraction reactions by H radicals are the fastest, an order of magnitude higher than those by OH radicals. These results point out the conditions in the very rich ($\Phi = 1.9$) premixed flame.

The overall rate of hydrogen abstraction reactions in the Utah heptane mechanism is determined mainly by the reactions of H radicals (Figure 6) in contrast to the Pitsch mechanism, in which the abstraction reactions by OH radicals contribute significantly to the total rate of hydrogen abstraction. The hydrogen abstraction reactions by H radicals are one order of magnitude faster than those by OH, O, and CH_3 radicals.

The LLNL reduced mechanism includes 13 abstractors for hydrogen abstraction reactions, and the rates of abstraction reactions for the premixed flame by the three most active abstractors are shown in Figure 6. The most powerful abstractor is again the H radical, due to the rich conditions. The OH radical also contributes significantly to the overall rate of hydrogen abstraction. Other abstractors, O, CH_3, HO_2, C_2H_5, C_2H_3, CH_3O, O_2, CH_3O_2, $C_7H_{15}OO$-1, $C_7H_{15}OO$-2, and $C_7H_{15}OO$-3, in order of their relative importance, contribute little toward the overall rate of hydrogen abstraction. A distinguishing feature of the LLNL mechanism is the abstraction reaction by the OH radical, the rates of which reach their maxima earlier in the flame, at a position where the temperature is around 800 K compared to 1270 K using either the Utah or the Pitsch mechanism. The earlier peak is the result of the bimodal shape of the OH radical profile as shown in Figure 7, although the concentration of OH radicals reaches its maximum later at 1570 K. Further studies indicate that the minor OH peak at 800 K is formed mainly by the low-temperature alkylperoxy chemistry, which will be discussed later and is a unique feature of the LLNL mechanism. The low-temperature chemistry in the LLNL mechanism is needed to capture the negative temperature coefficient (NTC) regime of hydrocarbon combustion. The first OH peak corresponds to the initiation of the NTC.

Fuel Consumption via Thermal Decomposition. *Thermal Decomposition in Premixed Flames.* Thermal decomposition provides an important fuel consumption route in addition to hydrogen abstraction, especially for diffusion flames.[14] Its importance in premixed flame, however, needs to be critically examined. The rates of thermal decomposition in the premixed flame are plotted in Figure 3, as well as the product distribution for each decomposition pathway. The Pitsch, Utah, and LLNL mechanisms include one (leading to C_4H_9-1 + n-C_3H_7), two (C_4H_9-1 + n-C_3H_7 and C_5H_{11}-1 + C_2H_5), and three (C_4H_9-1 + n-C_3H_7, C_5H_{11}-1 + C_2H_5 and C_6H_{13}-1 + CH_3) thermal decomposition reactions, respectively. The inclusion of one extra reaction gives a net rate of thermal decomposition in the Utah mechanism twice that given in the Pitsch mechanism. The minor reaction route $C_1 + C_6$ accounts for only 5% of the net rate of decomposition reactions in the LLNL mechanism, a route that leads to methyl radical formation. The temperatures at which the net rate of thermal decomposition exceeds that of hydrogen abstraction are 1400 K for the Utah, 1500 K for the Pitsch, and 1600 K for the LLNL mechanisms. At those high temperatures, however, less than 1% of the *n*-heptane fuel in the feed gas remains in the reaction mixture as seen in Table 3. The thermal decomposition accounts for 4%, 8%, and 0.4% of the total fuel consumption using the Pitsch, Utah, and LLNL mechanisms.

Thermal Decomposition in Opposed Diffusion Flames. The numerical results using the Pitsch mechanism in a diffusion flame are much different. At the flame front, the thermal decomposition rate matches those of hydrogen abstraction, as shown in Figure 4; i.e., the thermal decomposition rate of $C_3 + C_4$ exceeds the net formation rate of the primary heptyl radical via hydrogen abstraction (sum of four reactions with a peak of 1.01×10^{-4} mol/(cm^3 s)) at the position 0.46 cm from the fuel outlet (1300 K) and reaches a maximum rate (1.05×10^{-4} mol/(cm^3 s)) only 25% lower than the net formation rate (four reactions, 1.40×10^{-4} mol/(cm^3 s)) of the secondary heptyl radical. The three major fuel consumption pathways (hydrogen abstraction to the primary radical, hydrogen abstraction to the secondary radical, and thermal decomposition) represent a roughly 30/40−45/25−30% distribution of the fuel consumption at the flame front (0.45−0.48 cm from the fuel outlet). On the fuel side of the flame front, hydrogen abstraction is the principal fuel consumption route due to the low temperatures; on the oxidant side, hydrogen abstraction still dominates the fuel consumption due to higher abstractor concentrations.

Discussion

The competing pathways of fuel consumption are dominated by hydrogen abstraction and thermal decomposition. Hydrogen abstraction is the dominant fuel consumption route in premixed flames, only overtaken by thermal decomposition at temperatures higher than 1400−1500 K, where fuel concentrations are quite small. The principal abstractor is the H radical in all three mechanisms followed by OH and O radicals and other abstractors. Fuel consumption by thermal decomposition is insignificant in premixed flames due to the fuel depletion prior to reaching the decomposition temperature. Note that these conclusions depend on the very rich equivalence ratio and the premixed nature of the flame; it is very likely that reactions with OH would be the most important for flames close to stoichiometric conditions. In this sense, the reaction pathways depend on the equivalence ratio as well as the other important factors.

The LLNL mechanism shows a bimodal shape of hydrogen abstraction rates (Figure 6) because its OH profile features a minor peak at 800 K and a major peak near 1600 K (Figure 7). The OH concentration is about 5 orders of magnitude higher at 800 K using the LLNL mechanism than those obtained using the Pitsch and the Utah heptane mechanisms, which have little or no characterization of the low-temperature reactions. The

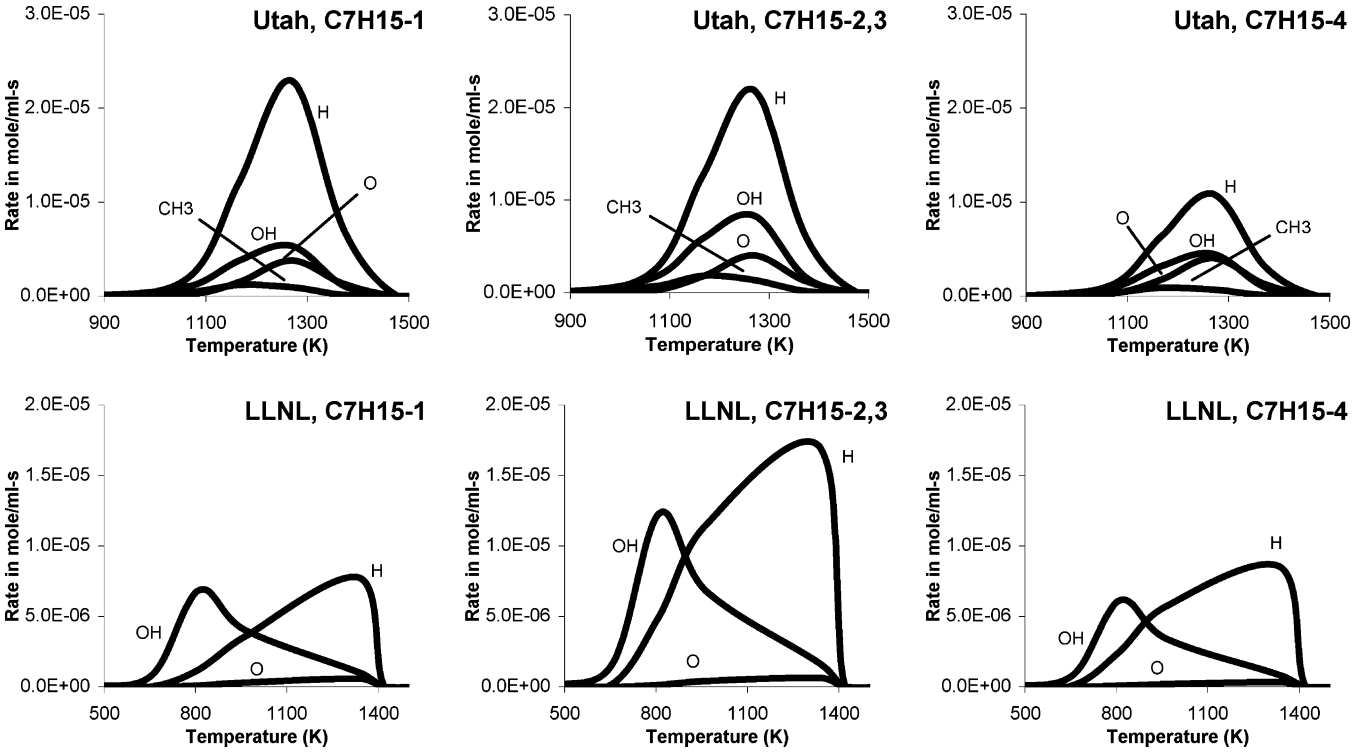

Figure 6. Hydrogen abstraction reaction rates in the premixed flame using the Utah (first row) and LLNL (second row) mechanisms. H, OH, O, and CH_3 are the hydrogen abstractors.

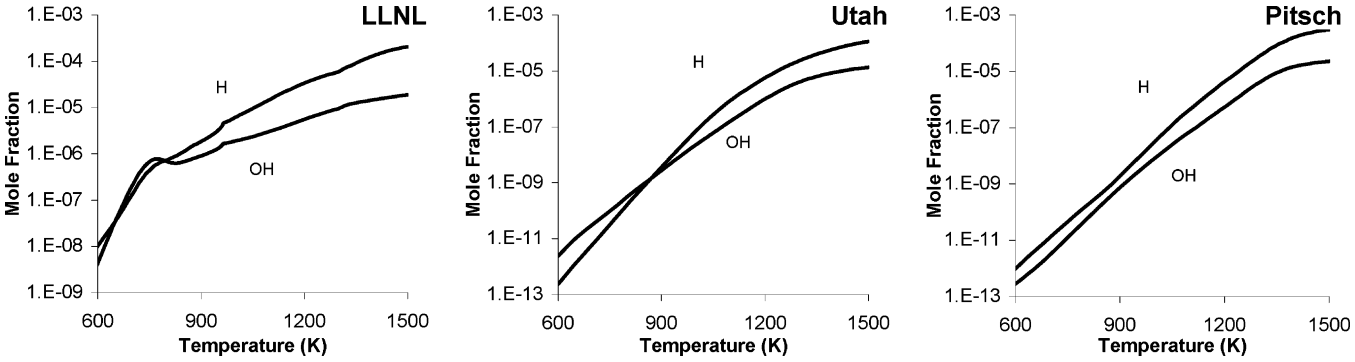

Figure 7. Concentration profiles of principal abstractors of hydrogen abstraction reactions in the premixed flame.

local OH peak concentration at 800 K results from the low-temperature peroxy chemistry, involving two decomposition reactions of hydroperoxy alkyl radicals and hydroperoxy alkyl peroxy radicals (using notations in the LLNL mechanism, $C_mH_{2m}OOH_{x-y} \Rightarrow C_mH_{2m}O_{x-y} + OH$ and $C_mH_{2m}OOH_{x-y}O_2 \Rightarrow nC_mket_{xy} + OH$). Details of the low-temperature chemistry are summarized elsewhere.[20]

Major fuel consumption pathways in the premixed normal heptane flame via thermal decomposition and hydrogen abstraction at 0.2 cm above the burner surface are elaborated in Figure 8, which also includes major isomerization reactions between conjugate alkyl radicals and their consecutive β scission reactions for the formation of olefins. The isomerization and β scission reactions were discussed in detail in an earlier publication.[45] Hydrogen abstraction dominates the fuel consumption (80.6%) in comparison with thermal decomposition (19.3%). The formation rate of the primary radical (21.4%) is approaching that of the secondary radicals (23.1% for C_7H_{15}-2/3 and 13.0% for C_7H_{15}-4) at a higher temperature (1270 K).

A more complete data set is presented in Table 3, which reports average fuel consumption distributions for the premixed flame for each spatial section. Let us examine as an example the importance of different pathways for the Utah mechanism. At heights above the burner (HAB) of 0.175 and 0.200 cm, the percentages of fuel remaining are 31.53% and 10.51%, respectively. The amount of fuel consumed in the interval HAB of 0.175−0.200 cm is 31.53−10.51% = 21.02%. From Figure 8, the fraction of the fuel consumed by hydrogen abstraction to yield C_7H_{15}-1 is 21.4% at HAB 0.200 cm. The corresponding value at HAB 0.175 cm (not provided) is 22.8%. The fractional contribution to the fuel consumption to form C_7H_{15}-1 in the HAB interval of 0.175−0.200 cm is therefore 21.02% × (22.8% + 21.4%)/2 = 4.65%. The integrated contribution of various channels, as sums of all sections, is also reported, and they add up to 92.27% for the Utah mechanism which is equal to the prediction by the mechanism for the fuel at the burner surface (92.33%). The deviation from the unity is due to experimental and simulation uncertainties and molecular diffusion. The gap, however, is not large. Therefore, a normalized distribution of different channels is also reported in Table 3. The thermal decomposition pathways accounts for only 4%, 8%, and 0.4% of the total fuel consumption in the Pitsch, Utah, and LLNL mechanisms. The primary radical formation accounts for 20−

Table 3. Percentage of Fuel Consumption for Different Product Channels

	Pitsch Mechanism				Utah Mechanism						
HAB[a]	fuel[b]	C_7H_{15}-1	(2,3 + 4) -C_7H_{15}	$C_3 + C_4$	fuel[b]	C_7H_{15}-1	C_7H_{15}-2	C_7H_{15}-3	C_7H_{15}-4	$C_2 + C_5$	$C_3 + C_4$
0.000	92.74%				92.33%						
0.025	89.42	0.52%	2.80%	0%	88.91	0.47%	1.16%	1.16%	0.62%	0.00%	0.00%
0.050	85.16	0.74	3.52	0	84.65	0.67	1.42	1.42	0.75	0.00	0.00
0.075	79.77	1.06	4.33	0	79.36	0.91	1.73	1.73	0.92	0.00	0.00
0.100	72.88	1.56	5.33	0	72.61	1.23	2.18	2.18	1.16	0.00	0.00
0.125	63.73	2.28	6.86	0.02	63.53	1.76	2.88	2.88	1.53	0.01	0.01
0.150	51.05	3.45	9.08	0.16	50.54	2.72	3.96	3.96	2.12	0.12	0.10
0.175	33.26	5.27	11.83	0.68	31.53	4.25	5.40	5.40	2.93	0.58	0.44
0.200	12.20	6.67	12.89	1.51	10.51	4.65	5.28	5.28	2.93	1.66	1.21
0.225	1.00	3.71	6.28	1.22	0.91	1.81	1.88	1.88	1.07	1.74	1.23
0.250	0.01	0.31	0.47	0.21	0.01	0.11	0.11	0.11	0.06	0.31	0.21
sum		25.56	63.39	3.80		18.58	26.00	26.00	14.08	4.41	3.20
normalized sum		27.56	68.34	4.09		20.14	28.18	28.18	15.26	4.78	3.46

	LLNL Mechanism							
HAB[a]	fuel[b]	C_7H_{15}-1	C_7H_{15}-2	C_7H_{15}-3	C_7H_{15}-4	$C_1 + C_6$	$C_2 + C_5$	$C_3 + C_4$
0.000	95.43%							
0.025	92.73	0.22%	0.99%	0.99%	0.50%	0.00%	0.00%	0.00%
0.050	88.59	0.41	1.49	1.49	0.75	0.00	0.00	0.00
0.075	82.16	0.77	2.27	2.27	1.13	0.00	0.00	0.00
0.100	71.88	1.47	3.53	3.53	1.76	0.00	0.00	0.00
0.125	56.65	2.43	5.12	5.12	2.56	0.00	0.00	0.00
0.150	41.11	2.49	5.23	5.23	2.61	0.00	0.00	0.00
0.175	26.71	2.19	4.89	4.89	2.44	0.00	0.00	0.00
0.200	11.33	2.24	5.26	5.26	2.62	0.00	0.00	0.00
0.225	0.48	1.59	3.56	3.56	1.78	0.02	0.18	0.15
0.250	0.00	0.07	0.14	0.14	0.07	0.00	0.03	0.02
sum		13.88	32.49	32.49	16.22	0.02	0.20	0.17
normalized sum		14.53	34.03	34.03	16.99	0.02	0.21	0.18

[a] Height above burner in centimeters. [b] Percent of the fuel remaining.

28% of the fuel consumption in the Pitsch and Utah mechanisms compared to 15% using the LLNL mechanism.

Hydrogen Abstraction in Opposed Diffusion Flames. The features of hydrogen abstraction in opposed diffusion flames can also be explained by the abstractor concentrations shown in Figure 9. The hydrogen radical reaches its maximum concentration at 0.53 cm from the fuel outlet (corresponding to a temperature of 1590 K), the OH radical, at 0.56 cm (1710 K), and the HO_2 radical (not shown), at 0.65 cm (1070 K). Hydrogen abstraction rates reach their maximum at the flame front around 0.48 cm from the fuel outlet (Figure 4), where the H radical concentration is 30−40 times that of the OH radical. The higher concentration of H radical in the flame zone determines its dominant role to form both the primary and secondary radicals (Figure 5). In contrast, hydrogen abstraction by OH in premixed flames is more important than in opposed diffusion flames as shown in Figure 5 as a consequence of the lower H/OH ratio, having values around eight. In the opposed diffusion flame, the maximum rates of abstraction reactions occur at 1390 K, 100−150 K higher than those in the premixed flame; therefore, the hydrogen abstraction reactions yielding the primary radical give a greater contribution to the fuel consumption with a net rate only 30% (Figure 4) lower than that of the secondary radical formation compared to 50% lower in the premixed flame (Figure 3) as a result of the enhanced formation rate of the primary radical at higher temperatures.

Relative Importance of Different Reaction Classes. *Relative Importance of Thermal Decomposition.* One contribution of this study is to clarify the importance of thermal decomposition in combustion of normal paraffins. These highly endothermic reactions gain importance only at high temperatures (1300−1400 K in premixed flames and around 1150 K in opposed diffusion flames). Thus, it is acceptable for these reactions to be excluded from mechanisms for low-temperature applications. Even in premixed flames, with temperatures increasing from 500−800 K at the burner surface to 1600−2000 K in the postflame zone, thermal decomposition is still of secondary importance (Table 3) relative to competing hydrogen abstraction since little fuel is left in the later flame zone where it is significant. However, this high-temperature reaction class may find its importance in many other applications. For example, in opposed diffusion flames, the fuel travels along the gas stream without significant decomposition until it approaches the flame front where the extensive heat released from the combustion makes thermal decomposition one of the principal consumption pathways of the fuel. It is the abundance of the fuel in the high-temperature region that is responsible for the importance of thermal decomposition that is comparable to hydrogen abstraction.

Relative Importance of Hydrogen Abstraction by OH Radicals. The reaction pathway analysis also provides insights into the relative importance of OH and H radicals in hydrogen abstraction. At low temperatures, the OH radical is more active than the H radical as seen in Figures 5 and 6. Hydrogen abstraction rates by OH radicals exceed those by H radicals when the temperature is lower than 1000 K in the Utah mechanism or lower than 1100 K in the Pitsch model. At high temperatures, the OH radical is usually of secondary importance to the H radical. Thus, hydrogen abstraction by the OH radical in high-temperature applications may be neglected or lumped into fewer reactions without significant impacts on the overall fuel consumption rate. Examination of the H/OH concentration ratio is the key in determining the relative importance of H and OH radicals, especially when H and OH radicals reach their maxima at different locations (Figure 9). Note that this conclusion depends very sensitively on the equivalence ratio of the flame. In the present case, the abstraction reactions with H atoms are dominant, but for flames closer to being stoichiometric, hydrogen abstractions via OH radicals are most important. This

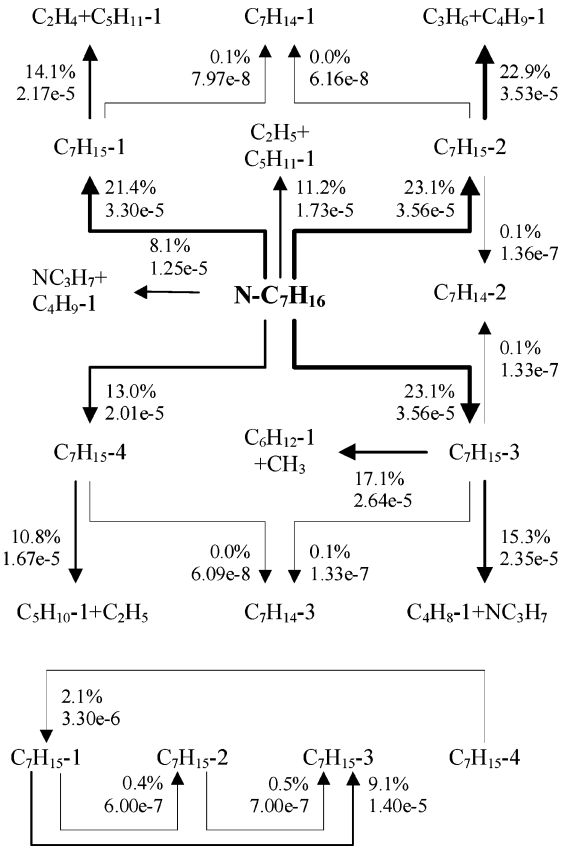

Figure 8. Product distribution in the premixed heptane flame at a position 0.2 cm above the burner surface using the Utah mechanism.

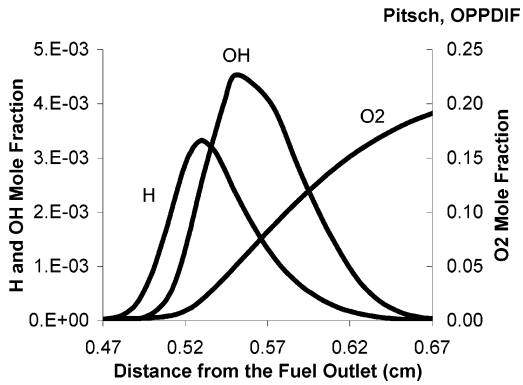

Figure 9. Concentration profiles of principal abstractors in hydrogen abstraction reactions in the opposed diffusion flame.

reinforces the point that mechanism reduction and reaction pathways are strong functions of the combustion equivalence ratios.

Relative Importance of Primary Alkyl Radical Formation. For some applications requiring small mechanisms, especially under low-temperature conditions, hydrogen abstraction forming conjugate primary radicals of the fuel may be neglected since those reactions are usually less important than those of secondary radicals. The temperature profile is the key in determining the importance of primary radical formation. If hydrogen abstraction reaches its maximum rate at higher temperatures, primary radical formation becomes more important, such as in Figure 4 for opposed diffusion flames. Another reason to neglect primary radical pathways is the relative abundance of secondary carbon, especially in higher paraffins such as *n*-decane (secondary/primary = 16/6), *n*-dodecane (20/6), and *n*-hexadecane (28/6). Furthermore, primary radicals decompose to ethylene molecules plus a smaller alkyl radical via cascading β scission reactions. Since β scission of large primary alkyl radicals is not a major formation pathway for ethylene,[45] the elimination of reactions forming conjugated primary radicals has even less impact on major species concentrations.

Mechanism Reduction. Reaction pathway analysis provides insights into the relative importance of competing reaction classes and provides a tool for tailoring mechanisms to specific applications. Insignificant reactions are eliminated or lumped into fewer reactions to facilitate faster numerical convergence and to make the model more applicable to a variety of simulation needs.

Figure 8 presents the product distribution for heptane decomposition in a premixed flame. The formation and consumption of the conjugate heptyl radicals at 0.2 cm above the burner surface are balanced, because the hydrogen abstraction step is controlling. For example, in Figure 8, the formation of the C_7H_{15}-3 radical accounts for 23.1% of the total fuel consumption, and this amount is distributed among the formation of C_6H_{12}-1 + CH_3 (17.1%) and C_4H_8-1 + NC_3H_7 (15.3%) via β scission and the formation of C_7H_{14}-3 via abstraction (0.1%). The decomposition of the C_7H_{15}-3 radical reflects an overconsumption of the C_7H_{15}-3 radical (32.5%) of three pathways. The gap (−9.4%) between the consumption and the formation via hydrogen abstraction from the fuel (23.1%) is filled by isomerization from C_7H_{15}-1 (9.1%) and C_7H_{15}-2 (0.5%). The decomposition of C_7H_{15} radicals, their balancing, and isomerization are discussed elsewhere.[45]

The balance between the formation and consumption of each conjugate alkyl radical provides a technique of mechanism reduction by lumping the two steps of hydrogen abstraction and consecutive decomposition into one reaction, e.g., *n*-C_7H_{16} + X = HX + C_4H_8-1 + *n*-C_3H_7. Generic rates of hydrogen abstraction, e.g., that of propane,[32] distinguished by primary and secondary carbons and adapted for the number of possible reaction sites, were used in many mechanisms. Such an approach, however, is not able to take into account isomerization reactions that may significantly shift the product distribution. An increase of the formation rate of C_7H_{15}-3 by as much as 50% is possible with isomerization.[45] Therefore, a more accurate product-distribution weighted approach is needed for better reproduction of olefin formation, which is critical for the formation of many soot precursors. Table 3 and its extension for scission product channels provide the necessary information for this approach as the formation rate of each product channel can be assigned as the total fuel consumption rate multiplying a weight function of product distribution. The total fuel consumption rate is the sum of rates via thermal decomposition, hydrogen abstraction for the primary radical, and hydrogen abstraction for the secondary radicals. The weight function is a regression fit of the temperature-dependent normalized product distribution for each channel, and the details of the reduction methodology will be presented in a future publication.

It is important to understand that reaction pathways and major product analysis depends quite sensitively on the conditions under which the fuel is burned. The differences observed above between premixed and non-premixed conditions depend considerably on the fact that fuel consumption in these two types of flames occurs under different kinetic regimes. The present premixed flame used for illustration is very rich, which emphasizes hydrogen abstraction reactions by H atoms. For flames close to being stoichiometric, abstractions by OH radicals are known to be much more important, and the resulting opportunities for mechanism reduction will therefore be much

different from those identified in the present rich combustion environment.

One observation that is important here is that the fully detailed, very extensive reaction mechanism is intended to describe all known conditions of fuel oxidation. This is the intent of the Curran et al.[20] mechanism; as a result, that kind of mechanism should be capable of simulating any set of conditions that can be used. Any type of mechanism reduction involves a suitable reduction in the set of conditions that can be described by the reduced mechanism, with the corresponding benefit of a reduction in the computational cost and complexity of the reaction mechanism and a lower computational cost of the model. Some reduction is simple, due to many reaction pathways that are never as important as others, and these can generally be eliminated at little cost or risk.

Other reductions depend on the operating conditions of the specific application of interest. Such conditions include the local equivalence ratio and operating temperatures and pressures. As shown above, the mechanism reduction suitable for diffusion flames might be much different from the reduction to accommodate premixed flames. The present work is intended to show how the reaction path analylsis tool is a very general type of analysis, but it can motivate and limit the subsequent type of mechanism reduction that would be most appropriate for the conditions being studied. In general terms, it suggests that the fully general reaction mechanism is an important tool from which reduced mechanisms can be generated, depending on the specific conditions being studied.

Conclusion

Pathway analysis is a useful tool in searching major reaction pathways in normal heptane flames. Hydrogen abstraction is identified to be the major fuel consumption pathway in premixed flames, and H and OH radicals are found to be the major abstractors. In determining the decomposition products, such as those shown in Figure 8, isomerization is important. The study underlines the greater importance of obtaining product distribution than kinetics of higher alkanes. The competing fuel consumption pathway via thermal decomposition becomes important at higher temperatures and makes a comparable contribution to the fuel consumption in opposed diffusion flames. Understanding the relative importance of competing pathways is an important step in mechanism reduction and generation.

Acknowledgment. This research was funded by the University of Utah (C-SAFE), through a contract with the Department of Energy, Lawrence Livermore National Laboratory (B341493).

EF060092Z